Scanning tunneling microscopy investigation of self-assembled poly(3-hexylthiophene) monolayer

Xiaojing Ma, Yan Guo, Tian Wang, and Zhaohui Su[a)]
State Key Laboratory of Polymer Physics and Chemistry, Changchun Institute of Applied Chemistry, Chinese Academy of Sciences, Changchun 130022, People's Republic of China

(Received 21 March 2013; accepted 29 May 2013; published online 1 July 2013)

Poly(3-hexylthiophene) (P3HT) monolayer has been investigated by scanning tunneling microscopy (STM). The monolayer was dominated by three kinds of ordered structure (I, II, and III), where the thiophene main chains lied parallel to one another, but high resolution STM images revealed that the arrangement of the hexyl side chains was different. In structure I, the hexyl side chains tilted at ∼60° with respect to the main chain, and the interchain distance (distance between two parallel neighboring backbones) was ∼1.41 nm. In structure II, the interchain distance was significantly larger at ∼1.52 nm, and the hexyl side chains were liquid-like. Structure III exhibited similar interchain distance as structure II, but the hexyl side chains were perpendicular to the main chain and were interdigitated. In addition to these ordered domains, individual poly(3-hexylthiophene) chains in various special configurations were observed, and their unfolding into more stable structures was tracked by dynamic STM, which provides evidence that P3HT is a relatively flexible polymer.
 [http://dx.doi.org/10.1063/1.4811236]

I. INTRODUCTION

Regioregular poly(3-alkylthiophene)s (P3ATs) have attracted a great deal of attention because of their high charge carrier mobilities, excellent processability, and environmental stability[1–3] that make them key materials used in plastic electronics, such as polymer solar cells and organic field-effect transistors (OFETs).[4–6] For these applications, the packing structure and side chain arrangement along the backbone of the conjugated polymers are crucial to their properties, for instance optical properties, conductivity and mobility.[2,7–10] In particular the device properties, such as the charge transport in OFETs, are governed by the structure of the first few molecular layers at the interface.[11,12] However, the structure of the interfacial layer in contact with the substrate is difficult to be assessed directly and is often inferred from the properties measured.[13–20] Furthermore, as semi-rigid conjugated polymers, the crystallization process and crystal structure of regioregular P3ATs are not well understood, in particular for poly(3-hexylthiophene) (P3HT), the most promising thiophene polymer for OFET and solar cell applications. Therefore understanding the intermolecular assembly behavior and intramolecular conformation of P3HTs at interfaces are of both fundamental and practical implications.

In recent years, diverse techniques, such as X-ray diffraction (XRD), nuclear magnetic resonance (NMR), and computer simulation, have been employed to explore detailed assembly behavior and crystal structures of P3ATs.[3,7,11–13] It has been established that P3AT molecules can assemble into layered structures composed of parallel stacks of thiophene main chains and alkyl side chains.[7,16,19–21] The conjugated polythiophene backbones are stacked together by the π-π interactions, whereas the side chains form nanodomains because of the phase separation between the rigid main chains and the flexible side chains.[3,22,23] Two kinds of crystal modification have been identified for P3ATs, Form I and Form II, which differ mainly in side chain arrangement and conformation.[3,7,21,24] It is widely accepted that in Form I, the side chains are tilted away from the plane of the conjugated backbones to eliminate alkyl chain interdigitation,[17] and in Form II, the side chains are interdigitated.[16,20,24,25] For P3HT the interlayer spacing of the well-organized lamellar in Form I and Form II are about 16.3 Å[8,19,22] and 11.8 Å,[26,27] respectively, as determined by XRD. Side chain arrangements in these crystal structures were proposed mainly based on the main chain spacing measured by XRD and computer simulations; however, direct evidence about the side chain structures is lacking because of the difficulty in growing P3AT single crystals and lack of enough diffraction data for the side chains.

Scanning tunneling microscopy (STM) is a powerful tool for investigating two-dimensional (2D) molecular arrangement on surface at sub-molecular level[28–30] and has been employed in the study of self-assembly structures of thiophene-based materials.[9,31–44] So far most of these studies were focused on oligothiophenes and their derivatives,[33–37,45–49] and few reported on surface assembly structure of the polymers, especially P3HT,[9,31,50,51] because their crystal or ordered assembly structures are much more difficult to obtain and control compared to oligothiophenes. Mena-Osteritz *et al.*[9,31] first reported STM investigation of the 2D crystal structures of P3HT and poly(3-dodecylthiophene) (P3DDT) at liquid/solid interface. The folding and assembly structure of the thiophene chains were first visualized and analyzed in conjunction with semiempirical calculation, and the interchain distances were measured directly from the STM images

a)Author to whom correspondence should be addressed. Electronic mail: zhsu@ciac.jl.cn

(about 1.3–1.4 nm for P3HT). After that, Grévin *et al.*[10,50] performed STM measurements on dried P3HT films and obtained size information of the crystalline domains (about 20 nm). Their results show that P3HT forms same assembly structures in dried films and at liquid/solid interface. However, arrangements of the alkyl side chains in these P3HT assembly structures were not well resolved and discussed.

In this paper, we present STM studies of self-assembled P3HT monolayer at the liquid/solid interface at submolecular resolution that enables identification of not only different assembly structures of P3HT in the monolayer but also different alkyl side chain arrangements and orientation for the first time. It is shown that different assembly structures at the interface can coexist. The movements and structural transformation of the P3HT chains are also studied by dynamic *in situ* measurements.

II. EXPERIMENTAL

Regioregular P3HT ($M_n = 16\,000$, PDI = 1.90) was purchased from Rieke Metals Inc. and used without further purification. Molecular weight was determined using gel permeation chromatography (GPC) with THF as the solvent and monodisperse polystyrene as standards. H-T regioregularity of the P3HT was measured by comparing the ratio of signals at 2.8 and 2.6 p.p.m. in NMR to be ~98%.[2] Toluene and 1-phenyloctane was purchased from Beijing Chemical Reagents Company and Aldrich, respectively. All the solvents were used as received without further purification.

The P3HTs were dissolved in toluene with a concentration of about 0.5 mg/ml. Samples for STM measurements were prepared by directly depositing a droplet (about 2 μl) of the P3HT solution on the surface of a freshly cleaved highly oriented pyrolytic graphite (HOPG, grade ZYB. Advanced Ceramics Inc., Cleveland, USA). 1-Phenyloctane was added between the tip and the sample surface to make the liquid/solid interface. STM measurements were performed both at the air/solid (without 1-phenyloctane) or liquid/solid (with 1-phenyloctane) interface, and same structures were observed but the presence of 1-phenyloctane resulted in better image quality. Therefore the data reported are for the P3HT monolayer at the liquid/solid interface.

STM measurements were performed at room temperature on a Bruker Nanoscope IIIA scanning tunneling microscopy system. The STM tips were mechanically cut from Pt/Ir wires (80%/20%). STM images were collected with the constant current mode and used with only flatten processing. The graphite substrate underneath the monolayer was recorded immediately after an image of the assembly was acquired by lowering the bias. The drift of the image was corrected using the Scanning Probe Image Processor (SPIP) software against the graphite lattice. The tunneling conditions of each STM image are given in the corresponding figure captions. The statistics of the contour length of the polymer chains were extracted from the images obtained at different sites of replicate samples to ensure the reliability. The construction and geometry optimization of the molecular models were performed with a HyperChem Pro 6.0 software package.

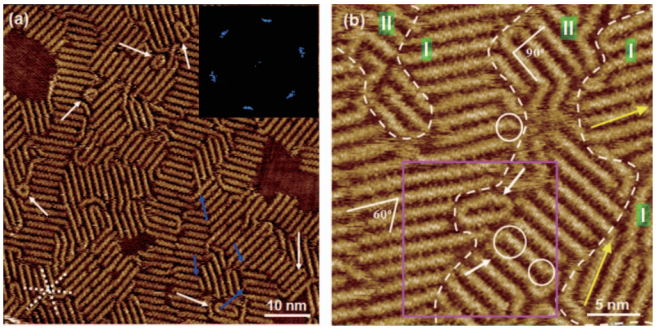

FIG. 1. (a) Large scale STM image of the monolayer formed by P3HT at the solution/HOPG interface. The star in the lower left corner indicates the threefold symmetry directions for the polymer ordering. The inset is the corresponding FFT of this image, which shows the threefold symmetry of the adlayer. The blue arrows mark the hairpin and folded structures with an angle of 60° or 120°. The white arrows indicate irregular special-shaped structures. (b) High-resolution STM image of the P3HT assembly structures. The dash lines outline domains of different structures (I and II). Higher resolution image of the area marked by purple square is shown in Fig. 2(a). The circles mark partial foldings in polymer chains, which contain thiophene units in *cis* conformation.[9] The tunneling conditions: (a) $V_{bias} = -230$ mV, $I_{tip} = 96$ pA; (b) $V_{bias} = -250$ mV, $I_{tip} = 92.34$ pA.

III. RESULTS AND DISCUSSION

Previous STM studies have demonstrated that thiophene-based conjugated molecules, including P3HT, can readily adsorb from dilute solution to HOPG surface and form a monolayer.[9,31,41,50,51] Figs. 1(a) and 1(b) are representative large-scale and high-resolution STM images, which show the long-range and short-range ordering of P3HT monolayer at the liquid/solid interface. It is obvious that P3HT molecules adsorb readily and form a stable close-packed monolayer, where parallel lamellae structures are clearly observed. In the P3HT monolayer, the conjugated backbones lie flat on the basal plane of the HOPG due to the π-π interactions between the conjugated backbones and the substrate, and the molecular chains align along the three crystallographic axes of the graphite lattice (marked by the white stars in Fig. 1(a)), which is also confirmed by the hexagonal spots in the fast Fourier transform (FFT) of the STM image (Fig. 1(a) inset). The bright features in the STM images should be correlated to the π-conjugated backbones of P3HT due to their higher electron density compared to the alkyl chains.[9,31,35,50–53] In Fig. 1(a), most of the P3HT molecules are in extended conformation or folded with an angle of 60° or 120° (some examples marked by the blue arrows). But occasionally some irregular special-shaped structures (marked by the white arrows) are also observed. This will be discussed in more detail later.

The high resolution STM image (Fig. 1(b)) reveals a distinct feature in P3HT assembly that was not reported before. There are two different assembly structures formed by P3HT, as differentiated by the white dotted lines in Fig. 1(b), referred to as structure I and structure II hereafter. It can be seen that in structure I the alkyl chains are titled with respect to the conjugated backbone with an angle of 60° ± 2°, while in structure II the side chains appear orienting perpendicular to the conjugated backbone. We will discuss this structure in more detail below. The average interchain distance in structures I

and II is measured to be 1.41 ± 0.02 nm and 1.52 ± 0.03 nm, respectively. Different orientation of the side chains with respect to the backbones should result in the change of the interchain distance (distance between neighboring backbones) in the monolayer, but it has been reported that this distance difference is usually too small to be distinguished by STM.[41] Here in our case, it can be clearly identified by measuring several parallel polymer chains, even though the interchain distances in the two assembly structures are also not too much different. It is worth noting that two structure I domains with different orientations have been observed (as marked by the yellow arrows in Fig. 1(b)), where the interchain distance measured was 1.41 ± 0.02 nm and 1.40 ± 0.02 nm, respectively, same within experimental error. This result suggests that neither the side chain conformation nor the interchain distance is due to epitaxy effect of the underlying graphite and depends on the orientation, and also confirms our measurement accuracy for the interchain distance.

To obtain more detailed packing information on structures I and II, a selected area in the high resolution STM image (Fig. 1(b)) is magnified and shown in Fig. 2(a), in which

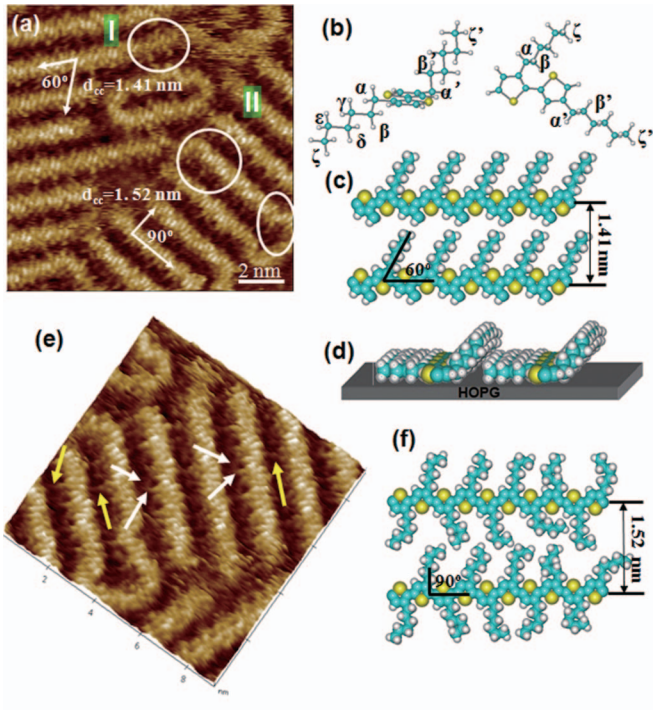

FIG. 2. (a) STM images of the short-range ordering of P3HT corresponding to the purple rectangle in Fig. 1(a). Tunneling conditions: $V_{bias} = -203.7$ mV, $I_{tip} = 119$ pA. The white circles indicate partial foldings in P3HT molecular chains. (b)–(d) and (f) Schematic models for different packing modes, which showed different side chains arrangements and orientation. (b) Side view of model of a bithiophene unit before (left) and top view of after (right) it adsorbs onto a surface. (c) Molecular arrangement model, in which the side chains on one side of the thiophene backbone are oriented at about 60° to the backbone. (d) Side view of the model in (c), where the side chains on one side of the main backbones are laid at the solution/HOPG interface and the alkyl chains on the opposite side are excluded from the surface and float in the solution. (e) 3D high resolution STM image corresponding to the right corner structures in (a). Arrows indicate different kinds of side chain arrangement: The white arrows mark neighboring side chains with chain ends tilting toward each other, and the yellow arrows mark interdigitated side chains. (f) Model for structure III, where the side chains are disordered.

how the alkyl chains orient with respect to the conjugated backbone and interdigitate in different assembly structures can be clearly distinguished. It can be seen that for structure I, located at the left in Fig. 2(a), the alkyl chains are aligned at an angle of about 60° ± 2° with respect to the backbone axis. In order to clarify how the alky chains are arranged at this angle after they adsorb from the solution onto the surface, a bithiophene unit model (Fig. 2(b)) was built and optimized using Hyperchem software. It should be emphasized that in linear sections of the chains the thiophene units adopt *trans* conformation, whereas *cis* conformation is only present in foldings or partial foldings (such as the ones marked by white circles in Figs. 1(b) and 2(a)).[9,10] Only the linear chain segments were concerned here, so *trans* conformation was assumed for all the units in the model, which means that all the alkyl side chains align alternatively along the conjugated backbone. The molecular model on the left in Fig. 2(b) illustrates the thiophene molecule in the liquid or gas phase (i.e., before it attaches onto the surface), where the side chains on both sides of the thiophene backbone are arranged in zigzag form to the backbone plane. When the molecule adsorbs from the solution onto the surface, the thiophene backbone lies flat on the basal plane of HOPG due to the π-π interactions between the thiophenes and the substrate, which forces part of the alkyl chain (β to ζ methylene units) previously tilting below the thiophene conjugation plane to rotate into a flat configuration on the HOPG surface, whereas the α and α' carbons stay in the same plane with the thiophenes in the process. Meanwhile the alkyl side chain on the opposite side remains in the liquid since it is located above the thiophene units. The molecular model on the right in Fig. 2(b) depicts the molecule after it adsorbs onto the HOPG surface, which shows that the alkyl chains orient from the thiophene main chain with a 60° angle. Such molecular conformation, where some alkyl chains lie flat on the substrate and others extend from the backbone and float above the surface, has been reported for oligothiophenes and is believed to reduce the steric hindrance in the monolayer.[34] Based on the above single thiophene unit model and STM observation, we propose an assembly model for structure I as shown in Figs. 2(c) (top view) and 2(d) (side view). Since the alky side chains floating in the liquid, which are better seen in the side view in Fig. 2(d), make no contribution to the STM image, the floating sections are omitted in Fig. 2(c) for simple presentation. The model best accommodates the key structure features observed by STM, ∼60° tilted side chain and an interchain distance of ∼1.41 nm, and its other features (e.g., main chain structure) are reasonable. Even though energetically this structure is not most favorable, since various structures co-existed in the monolayer (e.g., Fig. 1), indicating that the monolayer was not at thermodynamic equilibrium, some energetically less favorable structures such as this one can be present.

On the right in Fig. 2(a), detailed side chain arrangement in structures II is clearly resolved. The side chains appear to be perpendicular to the backbone in Fig. 1(b), where the scan area was greater than 25 nm across. However, in the magnified and 3D STM images of ultra-high resolution (Figs. 2(a) and 2(e)), it is interesting to see that not all the side chains are perpendicular to their backbones. In fact some of the side chains

are oriented rather arbitrarily. For example, some neighboring side chains are tilted to the backbone and bent toward each other to form circle-like structures (marked by white arrows in Fig. 2(e)); some side chains from neighboring backbones are interdigitated (marked by yellow arrows), and yet others orient with various angles. It is widely accepted that ordered P3HT structures consist of lamellae of stacks of the thiophene main chains with liquid-like side chains in between, and recent spectroscopic studies have further indicated that the side chains in P3HT can be disordered but are not completely liquid-like.[25,54–56] Our STM results provide for the first time direct observation of such kind of intermediate structure in between crystalline and liquid-like side chains in P3HT. It should be mentioned that because the alkyl side chains in structure II are not crystallized and remain somewhat mobile, it is very difficult to obtain a clearer image. More STM images containing structure II are included in the supplementary material.[57] Combining the ultra-high resolution STM images with the interchain distance (about 1.52 nm) in structure II, we propose a disordered side chain model for structure II, as illustrated in Fig. 2(f).

In addition to structures I and II discussed above, more careful analysis of the STM images reveals another ordered structure of P3HT in the monolayer, as shown in Figs. 3(a) and 3(b). Similar to Fig. 1(a), two kinds of side chain arrangement are also found to coexist in the monolayer. One of them is the previously observed structure I, in which the side chains align at an angle of 60° with respect to the backbone and the distance between two neighboring main chains in lamellae is 1.41 ± 0.02 nm. The other structure, here named as structure III, exhibits an average interchain distance of 1.51 ± 0.03 nm, same as that in structure II. However, the side chains in this structure are clearly interdigitated and aligned with an angle of 90° to the backbones. In contrast, the side chains in

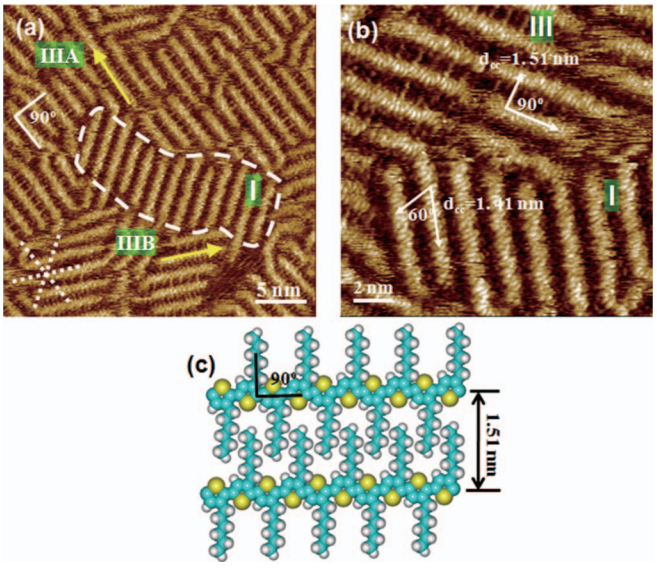

FIG. 3. STM images showing long-range (a) and short-range (b) ordering of P3HT. The white star indicates the threefold symmetry in the polymer ordering. The dash line marks two domains (I and II) with different assembly structure. Tunneling conditions: (a) $V_{bias} = -223$ mV, $I_{tip} = 90$ pA; (b) $V_{bias} = -201$ mV, $I_{tip} = 100$ pA. (c) Model of structure III in (a).

structure II are more disordered and liquid-like, although the interchain distance is the same as that for structure III. For this reason, it is not easy to distinguish these two structures in large-scale images (such as Fig. 1(b)), but in high resolution images their different side-chain arrangements are clearly distinguished. It is interesting to note that in all these images (Fig. 2(a) and Fig. S1 of the supplemental material), the side chains in structure III, which are crystallized, are clearly resolved, whereas most side chains in structure II are not. This observation indicates that the less clear resolution of the side chains in structure II is due to their inherent characteristic and not the data acquisition, i.e., the side chains in structure II are disordered, as we concluded above. It should also be noticed that in Fig. 3(a) the orientation of the two structure III domains (marked as IIIA and IIIB) is totally different, and the interchain distance is the same (1.52 ± 0.02 nm and 1.50 ± 0.03 nm, respectively), which further illustrates that the side chain arrangement is not a result of the epitaxy effect of the underlying substrate, as we have seen above with structure I.

Furthermore, the extend of side-chain interdigitation can be determined from the lamellar spacing and tilt angle of the side chains, which can be measured directly from the STM image, and structural parameters of the molecule.[25,58] Therefore, it can be calculated that in structure III, half length of the side chains are interdigitated with that from the neighboring P3HT chains. The corresponding model built by HyperChem software is shown in Fig. 3(c). By analyzing a large number of STM images obtained for different sites of many replicate samples, it was estimated that the area of structure III was about four times of structure I. The higher population of structure III may be attributed to its side chain interdigitation, which would increase interactions between adjacent P3HT molecules, making the structure energetically more favorable than structure I.

It is well known that due to its relatively stiff main chain P3HT forms layered crystalline structures; two crystal modifications have been identified as Form I and Form II, with layer spacing of about 1.6 and 1.2 nm, respectively.[7,8,16,19,22] Because it is difficult to grow P3HT single crystals, the side chain conformation in Form I and Form II structures have only been deduced and proposed based on distances between the backbones, which were calculated from diffraction data and simulation results.[16,24] In the structural model of Form II the side chains are interdigitated, whereas in that of Form I they are not interdigitated. For 2D P3HT assembly structures, the interchain distance was reported to be about 1.4 nm and the side chains were believed to interdigitate due to the strong interactions between P3HT with the substrate.[9,50] However, so far there has been little direct experimental evidence of these side chain structures and arrangements. Our STM studies have provided such evidence and show the coexistence of different assembly structures. We have directly observed hexyl side chains packing at an angle of 60° with respect to the main chain (structure I), side chains in disordered state (structure II), and side chains interdigitated with that from neighboring main chains (structure III). Previous study on thiophene oligomers has demonstrated that their 2D assembly structures exhibit similar or even same

characteristics with corresponding 3D structures.[59] In another word, the intrinsic characteristics of the 3D structures are preserved, but the exact parameter might vary after the molecules absorb onto the surface. Here in our case of P3HT polymer, compared to the crystal structures in the bulk, the 2D assembly structures of P3HT should be dominated by the interchain interactions as well as the interactions between P3HT and the underlying graphite substrate. Therefore, the interchain spacings we observed at the interface are different from that for Form I and Form II.

It has been found that in devices the interfacial layer of the P3HT films on the substrate has great effects on the device performance[11,12] and adsorption and assembly of P3HT on various dielectric substrates has been investigated by AFM and XRD.[13–15] The P3HT molecules can adopt either edge-on or face-on orientation with respect to the substrate according to the physical properties of the substrate and the sample processing conditions. However, the edge-on or face-on model was presumed based on average property values of the entire film and was difficult to be obtained directly. Here, STM images provide direct evidence of molecularly resolved assembling characteristics of the first interfacial layer of P3HT molecules on HOPG-liquid interface. It should be noted that submolecular resolutions have been demonstrated in earlier STM studies, where the folding and polycrystal structures of P3HT have been studied.[9,37] However, all previous STM studies on P3HT reported only one interchain distance value of ~1.4 nm[9,38] whereas in this work, a new spacing of ~1.5 nm was revealed in additional to the literature value. This may be ascribed to different extent of side chain interdigitation because of the mismatch between the P3HT and the substrate. Nevertheless, the assembly structures and side chain arrangement observed here provide valuable information on the ordered structures of P3HT at the interface.

Another observation of interest is that some domain boundaries between different phases in the STM images appear to be fuzzy, as seen in Figs. 1(b) and 3(b). One possible reason is rearrangement of P3HT molecules in the domain boundary areas: due to poor time resolution ability of STM technique in its standard mode, the dynamics of the rearrangement process cannot be captured.[60] Clearer images may be obtained by time-resolved STM.[60]

The submolecular resolution of these images makes it possible for us to identify individual P3HT chains and determine their contour lengths. Fig. 4 shows the distribution of the contour length of P3HT, which were obtained by measuring about 500 chains in images obtained from different areas of replicate samples. The average molecular weight can then be determined to be about 5800 from the contour length data in Fig. 4. This number-averaged molecular weight estimated by STM is apparently smaller than the GPC value (16 000). Similar phenomenon has been reported by others,[10,41] because GPC measurements of polythiophenes against polystyrene standard usually overestimate the molecular weight by a factor of 2–3.[10,41,61] Taking this factor into consideration, the molecular weight we obtained by STM in fact is in line with the GPC value.

It has been reported that chain foldings have significant influence on the electrical properties of the devices.[14]

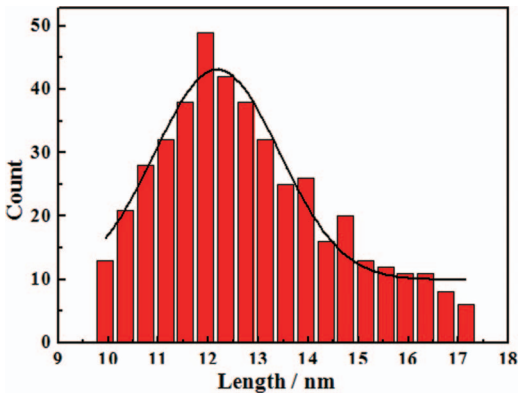

FIG. 4. Histogram shows the statistic of the contour length of the polymer chains in the assembling layer on the interface. The black line represents the Lorentz fit of the length distribution.

Our STM data have shown that over most of the surface, the adsorbed P3HT molecules assemble in linear, hairpin or normal folded (60°, 120°) structures. However, some special structures with uncommon shapes are occasionally observed, as shown in Fig. 1(a) and indicated by the white arrows. High resolution view of examples of these special structures is shown in Fig. 5. The shape of these structures varies; some of them appear "closed" (Figs. 5(a)–5(d)), whereas a gap can be clearly seen in others (Figs. 5(e)–5(h)). Polythiophenes are known as semi-rigid polymer with some flexibility, the monomer units in which can adopt both *trans* and *cis* conformations.[9] The thiophene units in P3AT are expected to adopt an all-*trans* conformation in linear chain sections, but they switch to a *cis* conformation at the elbow of bends or folds to reduce steric hindrance between neighboring thiophene units.[9] The energy for this switch is about 12–20 kJ/mol, if the substituent is on the β-position. Thus in principle, it is possible for P3HT to form structures with several folding points. It has been reported that sometimes oligothiophenes can absorb onto HOPG surfaces in the shape of a sinuous line, which makes the final assembly structure appear like a "wave."[34] Since *cis* conformation is prerequisite for the folds or bends, there has to be more *cis* conformers in these special circular structures to minimize steric hindrance. This means that most of the sulfur atoms are directed inside the cavity, and the alkyl chains are oriented outward, and thus cannot well interdigitate with one another to form ordered

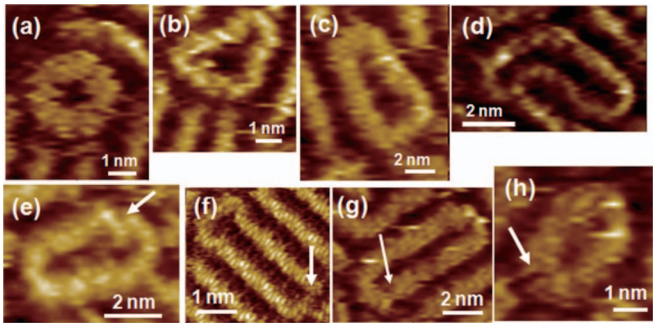

FIG. 5. (a)–(d) High resolution STM images of "closed" structures of various shapes. (e)–(h) Structures of special shape with gap clearly seen. The white arrows indicate the gaps.

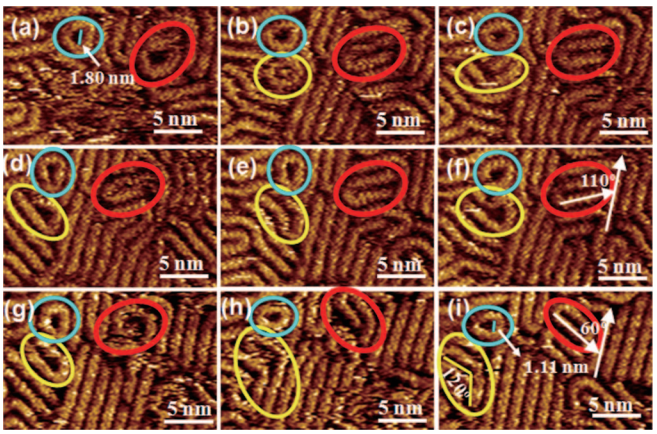

FIG. 6. Dynamic process of P3HT chain movement at the solution/solid interface. Cyan circles highlight the evolution of a "triangle" structure formed by one P3HT chain, yellow ellipses indicate a transformation from a "circle" structure to a "hairpin" structure, and red ellipses mark the change from a "circle" to hairpin structure.

crystal structures. Both the "*cis*" conformation of the thiophene units and the disordered alkyl side chains make these special structures higher energy states and thus less probable. In other words, the closed structures of P3HT are in general energetically less favorable due to bending energy penalty.

Under suitable conditions the energetically unfavorable structures are expected to transform into more stable structures over time. Fig. 6 displays a series of time-dependent STM images of a same area, recorded at 1 min interval, which reveal the dynamic process of structure evolution of P3HT chains. As can be seen in Fig. 6(a), in the upper left of the image, marked by a cyan circle is a chain in "triangle" configuration, which over time changes into a hairpin structure (Fig. 6(i)), resulting in a decrease in the distance between two folding points (marked by a cyan line) from 1.80 ± 0.02 nm to 1.11 ± 0.02 nm. This new shape the chain adopts favors side chain interdigitation and thus can lower the free energy, so that the structure becomes more stable compared to the starting triangle. The red ellipse in Fig. 6(a) marks a chain in "circle" configuration, which evolves into hairpin shape (Fig. 6(b)). The chain stays in this stable structure for a while, and then it further transforms into another hairpin, with a different orientation (Fig. 6(i)). In the latter process (Figs. 6(f)–6(i)) the angle between the long axis of the hairpin and the extended chains in parallel nearby changes from 110° to 60° (Figs. 6(f) and 6(i)), which suggests that this re-orientation is driven by interactions between the P3HT and the graphite surface, a piece of evidence that interactions between the molecules and the substrate play an important role in the assembly. The yellow ellipses in the images track a slow transformation of a circle structure into a folded structure with a folding angle of 120°. Looking at the entire experiment process, it is also noted that while the special structures evolve into more stable structures, the structures with chains in extended linear conformation (indicated by the white arrows) remain unchanged, a clear indication that they are more stable compared to the special structures such as triangles and circles. In another word, this dynamic process demonstrates that the closed ring structures are energetically unfavorable. Also from Figs. 6(a)–6(i), it can be concluded that the structures that appear to be closed (Figs. 5(a)–5(d)) in fact are formed by single P3HT molecules and are open, just the gap between the two ends are too small to be observed clearly. These dynamic movements of the P3HT molecules at the interface provide direct evidence that the P3HT chains are indeed quite flexible to form diverse configurations.

IV. CONCLUSION

We have investigated at the submolecular level side chain structure and main chain packing of P3HT at the liquid/solid interface using STM. Two distinct interchain distances were observed corresponding to different side chain arrangements. Based on the STM observations, three ordered structures (I, II, III) are identified, where main chains are parallel to one another, but side chain packing structure is different. Structure I is characterized by a 60° angle between the hexyl side chains and the main chain, and hence a smaller interchain distance. In structure II, the interchain distance is significantly larger, and the hexyl side chains are intermediate between ordered and liquid-like, consistent with recent spectroscopic studies of side chain structures in P3HT. Structure III exhibits similar interchain distance as structure II, but the hexyl side chains are perpendicular to the main chain and are interdigitated. This is the first time that side chain arrangement and orientation with respect to the backbone in P3HT is clearly observed. These direct observations provide strong evidence for the similar side chain packing models proposed for P3HT crystal structures, and shed light on the interfacial structure of P3HT on dielectric substrates. In addition, individual P3HT chains in various special configurations have been observed, and their unfolding tracked by dynamic STM, which afford further evidence that P3HT is a relatively flexible polymer. These findings provide valuable information for understanding packing and crystal structures of P3HT, and P3ATs in general.

ACKNOWLEDGMENTS

This work is supported by National Natural Science Foundation of China (Grant No. 20990233) and the Scientific Research Foundation for the Returned Overseas Chinese Scholars, State Education Ministry. Z.S. thanks the National Science Foundation of China (NSFC) Fund for Creative Research Groups (Grant No. 50921062) for support. The authors thank Professor Yanlian Yang and Professor Qian Wang for helpful suggestions.

[1]H. Sirringhaus, N. Tessler, and R. H. Friend, Science **280**, 1741 (1998).
[2]H. Sirringhaus, P. J. Brown, R. H. Friend, M. M. Nielsen, K. Bechgaard, B. M. W. Langeveld-Voss, A. J. H. Spiering, R. A. J. Janssen, E. W. Meijer, P. Herwig, and D. M. de Leeuw, Nature (London) **401**, 685 (1999).
[3]O. F. Pascui, R. Lohwasser, M. Sommer, M. Thelakkat, T. Thurn-Albrecht, and K. Saalwachter, Macromolecules **43**, 9401 (2010).
[4]G. Li, V. Shrotriya, J. S. Huang, Y. Yao, T. Moriarty, K. Emery, and Y. Yang, Nat. Mater. **4**, 864 (2005).
[5]S. R. Forrest, Nature (London) **428**, 911 (2004).
[6]Y. Kim, S. Cook, S. M. Tuladhar, S. A. Choulis, J. Nelson, J. R. Durrant, D. D. C. Bradley, M. Giles, I. Mcculloch, C. S. Ha, and M. Ree, Nat. Mater. **5**, 197 (2006).

[7]T. J. Prosa, M. J. Winokur, and R. D. McCullough, Macromolecules **29**, 3654 (1996).
[8]R. D. Mccullough, S. Tristramnagle, S. P. Williams, R. D. Lowe, and M. Jayaraman, J. Am. Chem. Soc. **115**, 4910 (1993).
[9]E. Mena-Osteritz, A. Meyer, B. M. W. Langeveld-Voss, R. A. J. Janssen, E. W. Meijer, and P. Bauerle, Angew. Chem., Int. Ed. **39**, 2680 (2000).
[10]B. Grevin, P. Rannou, R. Payerne, A. Pron, and J. P. Travers, J. Chem. Phys. **118**, 7097 (2003).
[11]S. H. Wang, A. Kiersnowski, W. Pisula, and K. Mullen, J. Am. Chem. Soc. **134**, 4015 (2012).
[12]R. J. Kline, M. D. Mcgehee, and M. F. Toney, Nat. Mater. **5**, 222 (2006).
[13]D. H. Kim, Y. Jang, Y. D. Park, and K. Cho, Macromolecules **39**, 5843 (2006).
[14]T. C. Anglin, J. C. Speros, and A. M. Massari, J. Phys. Chem. C **115**, 16027 (2011).
[15]Y. Sun, J. G. Liu, Y. H. Geng, and Y. C. Han, Chin. J. Appl. Chem. **29**, 1399 (2012).
[16]K. Tashiro, M. Kobayashi, T. Kawai, and K. Yoshino, Polymer **38**, 2867 (1997).
[17]Z. Y. Wu, A. Petzold, T. Henze, T. Thurn-Albrecht, R. H. Lohwasser, M. Sommer, and M. Thelakkat, Macromolecules **43**, 4646 (2010).
[18]K. Yazawa, Y. Inoue, T. Yamamoto, and N. Asakawa, Phys. Rev. B **74**, 094204 (2006).
[19]T. J. Prosa, M. J. Winokur, J. Moulton, P. Smith, and A. J. Heeger, Macromolecules **25**, 4364 (1992).
[20]M. Mas-Torrent and C. Rovira, Chem. Rev. **111**, 4833 (2011).
[21]M. Brinkmann, J. Polym. Sci., Part B: Polym. Phys. **49**, 1218 (2011).
[22]T. A. Chen, X. M. Wu, and R. D. Rieke, J. Am. Chem. Soc. **117**, 233 (1995).
[23]Z. Bao, A. Dodabalapur, and A. J. Lovinger, Appl. Phys. Lett. **69**, 4108 (1996).
[24]G. H. Lu, L. G. Li, and X. N. Yang, Macromolecules **41**, 2062 (2008).
[25]R. J. Kline, D. M. DeLongchamp, D. A. Fischer, E. K. Lin, L. J. Richter, M. L. Chabinyc, M. F. Toney, M. Heeney, and I. McCulloch, Macromolecules **40**, 7960 (2007).
[26]J. G. Liu, Y. Sun, X. A. Gao, R. B. Xing, L. D. Zheng, S. P. Wu, Y. H. Geng, and Y. C. Han, Langmuir **27**, 4212 (2011).
[27]A. Zen, M. Saphiannikova, D. Neher, J. Grenzer, S. Grigorian, U. Pietsch, U. Asawapirom, S. Janietz, U. Scherf, I. Lieberwirth, and G. Wegner, Macromolecules **39**, 2162 (2006).
[28]Y. L. Yang and C. Wang, Chem. Soc. Rev. **38**, 2576 (2009).
[29]L. J. Wan, Acc. Chem. Res. **39**, 334 (2006).
[30]X. J. Ma, Y. B. Li, X. H. Qiu, K. Q. Zhao, Y. L. Yang, and C. Wang, J. Mater. Chem. **19**, 1490 (2009).
[31]E. Mena-Osteritz, Adv. Mater. **14**, 609 (2002).
[32]A. Gesquiere, P. Jonkheijm, F. J. M. Hoeben, A. Schenning, S. De Feyter, F. C. De Schryver, and E. W. Meijer, Nano Lett. **4**, 1175 (2004).
[33]M. M. S. Abdel-Mottaleb, G. Gotz, P. Kilickiran, P. Bauerle, and E. Mena-Osteritz, Langmuir **22**, 1443 (2006).
[34]Z. Y. Yang, H. M. Zhang, C. J. Yan, S. S. Li, H. J. Yan, W. G. Song, and L. J. Wan, Proc. Natl. Acad. Sci. U.S.A. **104**, 3707 (2007).
[35]L. P. Xu, J. R. Gong, L. J. Wan, T. G. Jiu, Y. L. Li, D. B. Zhu, and K. Deng, J. Phys. Chem. B **110**, 17043 (2006).
[36]T. Jaroch, R. Nowakowski, M. Zagorska, and A. Pron, J. Phys. Chem. C **114**, 13967 (2010).
[37]L. Wang, B. J. V. Tongol, S. L. Yau, T. Otsubo, and K. Itaya, Langmuir **26**, 7148 (2010).
[38]H. Zhang, F. J. M. Hoeben, M. J. Pouderoijen, A. P. H. L. Schenning, E. W. Meijer, F. C. De Schryver, and S. De Feyter, Chem.-Eur. J. **12**, 9046 (2006).
[39]F. J. M. Hoeben, J. Zhang, C. C. Lee, M. J. Pouderoijen, M. Wolffs, F. Wuerthner, A. P. H. J. Schenning, E. W. Meijer, and S. De Feyter, Chem.-Eur. J. **14**, 8579 (2008).
[40]Z. Guo, I. De Cat, B. Van Averbeke, J. Lin, G. Wang, H. Xu, R. Lazzaroni, D. Beljonne, E. W. Meijer, A. P. H. J. Schenning, and S. De Feyter, J. Am. Chem. Soc. **133**, 17764 (2011).
[41]S. B. Lei, K. Deng, Y. L. Yang, Q. D. Zeng, C. Wang, Z. Ma, P. Wang, Y. Zhou, Q.-L. Fan, and W. Huang, Macromolecules **40**, 4552 (2007).
[42]S. S. Jester, A. Idelson, D. Schmitz, F. Eberhagen, and S. Hoeger, Langmuir **27**, 8205 (2011).
[43]K. Yoosaf, A. R. Ramesh, J. George, C. H. Suresh, and K. G. Thomas, J. Phys. Chem. C **113**, 11836 (2009).
[44]S. B. Lei, L. J. Wan, C. Wang, and C. L. Bai, Adv. Mater. **16**, 828 (2004).
[45]Z. Y. Yang, H. M. Zhang, G. B. Pan, and L. J. Wan, ACS Nano **2**, 743 (2008).
[46]L. Piot, F. Silly, L. Tortech, Y. Nicolas, P. Blanchard, J. Roncali, and D. Fichou, J. Am. Chem. Soc. **131**, 12864 (2009).
[47]J. M. MacLeod, O. Ivasenko, C. Fu, T. Taerum, F. Rosei, and D. F. Perepichka, J. Am. Chem. Soc. **131**, 16844 (2009).
[48]E. Mena-Osteritz and P. Bauerle, Adv. Mater. **18**, 447 (2006).
[49]T. Jaroch, M. Knor, R. Nowakowski, M. Zagorska, and A. Pron, Phys. Chem. Chem. Phys. **10**, 6182 (2008).
[50]B. Grevin, P. Rannou, R. Payerne, A. Pron, and J. P. Travers, Adv. Mater. **15**, 881 (2003).
[51]A. Bocheux, I. Tahar-Djebbar, C. Fiorini-Debuisschert, L. Douillard, F. Mathevet, A. J. Attias, and F. Charra, Langmuir **27**, 10251 (2011).
[52]M. Brun, R. Demadrille, P. Rannou, A. Pron, J. P. Travers, and B. Grevin, Adv. Mater. **16**, 2087 (2004).
[53]P. Samori, V. Francke, K. Mullen, and J. P. Rabe, Chem.-Eur. J. **5**, 2312 (1999).
[54]M. C. Gurau, D. M. Delongchamp, B. M. Vogel, E. K. Lin, D. A. Fischer, S. Sambasivan, and L. J. Richter, Langmuir **23**, 834 (2007).
[55]Y. Guo, Y. Jin, and Z. H. Su, Soft Matter **8**, 2907 (2012).
[56]Y. Guo, Y. Jin, and Z. H. Su, Poly. Chem. **3**, 861 (2012).
[57]See supplementary material at http://dx.doi.org/10.1063/1.4811236 for more STM images.
[58]D. M. DeLongchamp, R. J. Kline, E. K. Lin, D. A. Fischer, L. J. Richter, L. A. Lucas, M. Heeney, I. McCulloch, and J. E. Northrup, Adv. Mater. **19**, 833 (2007).
[59]R. Azumi, G. Götz, T. Debaerdemaeker, and P. Bäuerle, Chem.-Eur. J. **6**, 735 (2000).
[60]A. van Houselft and H. J. W. Zandvliet, Rev. Mod. Phys. **82**, 1593, (2010).
[61]J. Liu, R. S. Loewe, and R. D. McCullough, Macromolecules **32**, 5777 (1999).